



## 1 Stratospheric ozone depletion inside the volcanic plume shortly after the 2 2022 Hunga Tonga eruption

3  
4 Yunqian Zhu<sup>1,2,3</sup>, Robert W. Portmann<sup>1</sup>, Douglas Kinnison<sup>4</sup>, Owen Brian Toon<sup>3,5</sup>, Luis Millán<sup>6</sup>,  
5 Jun Zhang<sup>4</sup>, Holger Vömel<sup>7</sup>, Simone Tilmes<sup>4</sup>, Charles G. Bardeen<sup>4</sup>, Xinyue Wang<sup>4</sup>, Stephanie  
6 Evan<sup>8</sup>, William J. Randel<sup>4</sup>, Karen H. Rosenlof<sup>1</sup>

- 7
- 8 1. NOAA, Chemical Sciences Laboratory
- 9 2. Cooperative Institute for Research in Environmental Sciences, University of Colorado  
10 Boulder
- 11 3. Laboratory for Atmospheric and Space Physics, University of Colorado Boulder
- 12 4. NCAR, Atmospheric Chemistry Observations and Modeling Laboratory
- 13 5. Department of Atmospheric and Oceanic Sciences, University of Colorado Boulder
- 14 6. Jet Propulsion Laboratory, California Institute of Technology, 4800 Oak Grove Drive,  
15 Pasadena, CA 91109, USA
- 16 7. NCAR, Earth Observing Laboratory
- 17 8. Laboratoire de l'Atmosphère et des Cyclones (LACy, UMR8105, CNRS, Université de La  
18 Réunion, Météo-France), Saint-Denis, France

19  
20 Corresponding author: Yunqian Zhu (yunqian.zhu@noaa.gov)

### 21 22 **Abstract**

23 In-plume ozone depletion was observed for about ten days by Microwave Limb Sounder  
24 (Aura/MLS) right after the January 2022 Hunga Tonga-Hunga Ha'apai (HTHH) eruption. This  
25 work analyzes the dynamic and chemical causes of this ozone depletion. The results show that  
26 the large water injection (~150 Tg) from the HTHH eruption, with ~0.0013 Tg injection of ClO  
27 (or ~0.0009 Tg of HCl), causes ozone loss due to strongly enhanced HOx and ClOx cycles and  
28 their interactions. Aside from the gas phase chemistry, the heterogeneous reaction rate for  
29 HOCl+HCl→Cl<sub>2</sub>+H<sub>2</sub>O increases to 10<sup>4</sup> cm<sup>-3</sup>sec<sup>-1</sup> and is a major cause of chlorine activation,  
30 making this event unique compared with the springtime polar ozone depletion where  
31 HCl+ClONO<sub>2</sub> is more important. The large water injection causes relative humidity over ice to  
32 increase to 70% - 100%, decreases the H<sub>2</sub>SO<sub>4</sub>/H<sub>2</sub>O binary solution weight percent to 35%  
33 compared with the 70% ambient value, and decreases the plume temperature by 2-6 K. These  
34 changes lead to high heterogeneous reaction rates. Plume lofting of ozone-poor air is evident  
35 during the first two days after the eruption, but ozone concentrations quickly recover because its  
36 chemical lifetime is short at 20 hPa. With such a large seawater injection, we expect that ~5 Tg  
37 Cl was lifted into the stratosphere by the HTHH eruption in the form of NaCl, but only ~0.02%  
38 of that remained as active chlorine in the stratosphere. lightning NOx changes are probably not  
39 the reason for the HTHH initial in-plume O<sub>3</sub> loss.

### 40 41 **Key points:**

- 42 • HOCl is identified as playing a large role in the in-plume chlorine balance and  
43 heterogeneous processes, making this event unique compared with the ozone hole where  
44 HCl+ClONO<sub>2</sub> is more important.
- 45 • The HTHH eruption enhanced the HOx/ClOx cycles and their interactions, which caused  
46 in-plume O<sub>3</sub> depletion.



- 47 • The injection of Cl, H<sub>2</sub>O, and lightning NO<sub>x</sub> modified the ambient chemistry.

48

49

## 1. Introduction

50

Stratospheric ozone concentrations change after volcanic eruptions for a variety of reasons.

51

Enhanced polar ozone depletion occurs after large or medium volcanic eruptions [Hofmann and

52

Oltmans, 1993; Portmann *et al.*, 1996; Solomon *et al.*, 2016] since heterogeneous reactions on

53

volcanically enhanced sulfate aerosols result in amplified anthropogenic ClO<sub>x</sub> and BrO<sub>x</sub> induced

54

ozone loss. Tie and Brasseur [1995] demonstrated that mid- and high latitude O<sub>3</sub> changes after a

55

volcanic eruption largely depend on chlorine loading. For the pre-industrial era and in the

56

absence of anthropogenic halogens in the stratosphere, O<sub>3</sub> would slightly increase in the middle

57

atmosphere after a large volcanic eruption resulting from the suppression of NO<sub>x</sub>-catalyzed

58

destruction by heterogeneous creation of HNO<sub>3</sub> on volcanic aerosols. After the 1991 Pinatubo

59

eruption, the radiative heating caused by volcanic aerosols perturbed the local temperature and

60

circulation, which lifted the ozone layer and caused equatorial ozone depletion [Kinnison *et al.*,

61

1994]. Wang *et al.* [2022] reported that, in the case of the Hunga-Tonga eruption, mid-latitude

62

ozone reduction was primarily caused by anomalous upwelling. Enhanced water can also change

63

O<sub>3</sub>. In the lower most stratosphere, H<sub>2</sub>O injection through deep convection or tropopause cirrus

64

clouds could change the catalytic chlorine/bromine free-radical chemistry and shift the total

65

available inorganic chlorine towards the catalytically active free-radical form, ClO [Solomon *et*

66

*al.*, 1997; Anderson *et al.*, 2012].

67

Evan *et al.* [2023, submitted] report observations of decreased O<sub>3</sub> and HCl, and increased

68

ClO in the first week following the HTHH eruption at 20 hPa. Here we use the

69

CESM2(WACCM6) model [Zhu *et al.*, 2022] to analyze the dynamic and chemical contributors

70

to this initial in-plume ozone depletion. A lofting plume can bring ozone-poor tropospheric air

71

into the stratosphere and cause in-plume low ozone values compared with the surrounding

72

stratospheric air [Yu *et al.*, 2019]. For a submarine volcanic eruption, the in-plume air

73

composition is not only impacted by tropospheric air, but also by the seawater, and volcanic

74

gases (including H<sub>2</sub>O, CO<sub>2</sub>, SO<sub>2</sub>, HCl, HF, H<sub>2</sub>S, S<sub>2</sub>, H<sub>2</sub>, CO, and SiF<sub>4</sub>), and volcanic minerals.

75

For the HTHH initial plume, besides high H<sub>2</sub>O and high SO<sub>2</sub>, Microwave Limb Sounder (MLS)

76

observations indicate the in-plume air carried high CO (**Figure A1**), relatively low ozone, and

77

high ClO, compared with the surrounding air. We constrain the initial plume chemical

78

compounds based on observational data from MLS; then analyze how stratospheric chemistry

79

changes the plume composition. We will answer the following scientific questions:

80

1. What are the initial conditions in the volcanic plume?

81

2. What are the main causes of in-plume ozone depletion?

82

3. How do volcanic injections impact heterogeneous reactions that cause chlorine activation

83

in the plume?

84

85

## 2. Observational data description and model setup

86

The MLS instrument onboard the EOS Aura satellite was launched into a near-polar sun-

87

synchronous orbit in 2004. This work uses MLS version 4 for O<sub>3</sub>, ClO, temperature, and CO data

88

during the first ten days after the eruption as recommended by Millán *et al.* [2022]. The vertical

89

resolution of these MLS products is typically around 3-5 km in the stratosphere. All data used

90

here were screened using the methodology indicated in Livesey *et al.* [2022]. We use the MLS

91

H<sub>2</sub>O data to identify the plume location and define it as regions with water vapor larger than 10

92

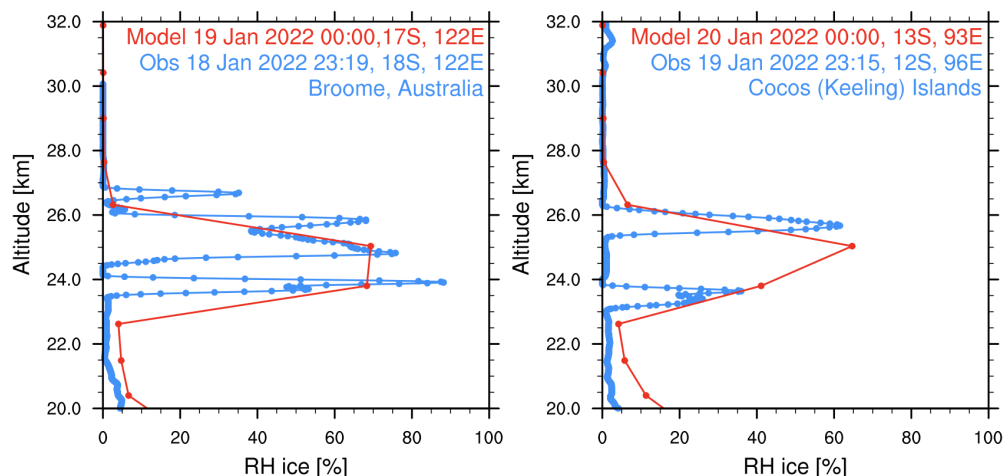
ppmv.



93 *Vömel et al.* [2022] provide water vapor radiosonde measurements during the first three  
 94 global circumnavigations of the plume. Here we calculate the relative humidity relative to ice  
 95 (RH<sub>i</sub>) and compare the observed values with the simulated values.

96 We use the 70-layer Whole Atmosphere Community Climate Model (WACCM) model as  
 97 described in *Zhu et al.* [2022], injecting SO<sub>2</sub> (0.42 Tg) and H<sub>2</sub>O (150 Tg). The model's vertical  
 98 resolution is about 1 km in the stratosphere. The model atmosphere is nudged to GEOS5  
 99 meteorological analysis [*Rienecker et al.*, 2008] until January 14, one day before the eruption  
 100 day. After January 15, we run the model freely with a fully interactive atmosphere and ocean for  
 101 ten days.

102 We constrain the simulated volcanic aerosol, H<sub>2</sub>O, and chlorine by comparing to  
 103 observations during the first ten days after the eruption. *Zhu et al.* [2022] show that the simulated  
 104 aerosol backscatter coefficient agrees with the CALIPSO observations on January 17. The  
 105 simulated H<sub>2</sub>O agrees with MLS [*Millán et al.*, 2022; *Zhu et al.*, 2022] from February 1 to April  
 106 1, 2022. Here, we compare the simulated H<sub>2</sub>O with the radiosonde observations of humidity  
 107 [*Vömel et al.*, 2022] during the first week. **Figure 1** shows the RH<sub>i</sub> on January 18 and January 19  
 108 observed by the radiosonde and from nearby simulated model output. Both the observations and  
 109 simulations show relative humidity between 70% to 100%. The radiosonde observations have a  
 110 much higher vertical resolution than the model. Therefore, they show multiple layers of water  
 111 enhancement, while the model only shows one.

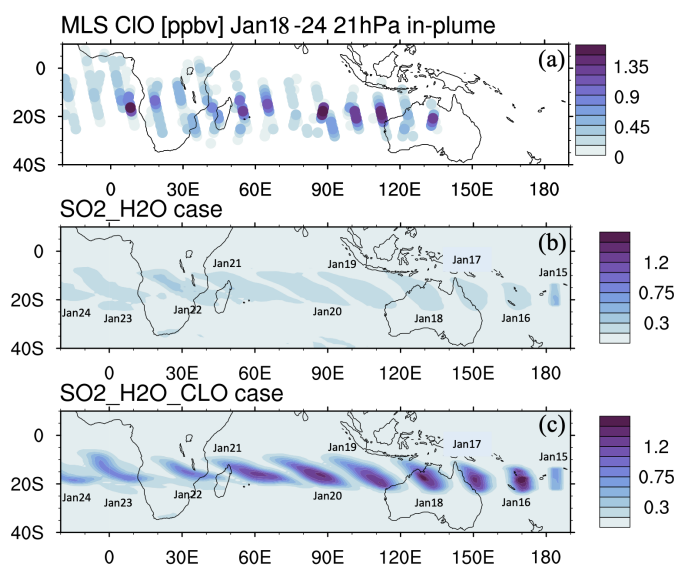


112 **Figure 1.** Relative humidity with respect to ice saturation vapor pressure from radiosondes (blue)  
 113 [*Vömel et al.*, 2022] and simulation (red). The profiles are picked at nearby locations. Note the  
 114 observations are about 45 minutes earlier in time than the simulations, which places them on a  
 115 different day.  
 116  
 117

118 We constrain the chlorine injection using MLS ClO observations at 20 hPa. **Figure 2a**  
 119 shows ClO from the MLS observations and the model simulations at 20 hPa from January 18 to  
 120 January 24. MLS values are selected from locations where water vapor is larger than 10 ppmv,  
 121 indicating these values are inside the volcanic plume. **Figures 2b** and **2c** show the simulated  
 122 daytime ClO for one plume location for each day. The dates are marked next to each plume.  
 123 MLS observations show elevated ClO, about 5 to 10 times higher than the ambient values  
 124 (**Figure 2a**). If we only inject SO<sub>2</sub> and H<sub>2</sub>O (The H<sub>2</sub>O\_SO<sub>2</sub> case defined in Table 1), we get a



125 ClO amount about twice as large as the background (**Figure 2b**), which is much lower than  
 126 observed. The change of ClO indicates that H<sub>2</sub>O alters the Cly partitioning. To match the  
 127 observed values, we need to inject 0.0013 Tg of ClO (**Figure 2c**). This is equivalent to injecting  
 128 ~0.0009 Tg of HCl (**Figure A2**). In our simulations, injecting ClO and HCl does not lead to  
 129 different HOCl (**Figure A3**), ClO, and O<sub>3</sub> levels after January 15, indicating the balancing of  
 130 ClO and HCl inside the HTHH plume happens very quickly. Unfortunately, the HOCl retrieval  
 131 from MLS is not suitable for scientific use at this pressure level, so we cannot validate it. We  
 132 choose the ClO injection case in our following analysis. Note that the MLS ClO vertical  
 133 resolution is ~2 km near 20 hPa, which is coarser than the model vertical resolution (~1 km at 20  
 134 hPa).  
 135



136  
 137 **Figure 2.** a) MLS in-plume ClO observations during the first 10 days after the eruption. “In-  
 138 plume” is defined as the area with water vapor mixing ratios larger than 10 ppmv. MLS in-plume  
 139 ClO data is not recommended for scientific use until January 18, 2022. b) and c) Simulated 10-  
 140 day evolution of in-plume ClO in the SO<sub>2</sub>\_H<sub>2</sub>O and SO<sub>2</sub>\_H<sub>2</sub>O\_CLO case. The modeled ClO  
 141 concentrations are only taken during daytime each day (either 6 UTC or 12 UTC).  
 142

143 To investigate the O<sub>3</sub> decrease and its related chemical evolution during the first 10 days,  
 144 we conduct several simulations as described in **Table 1**.  
 145

146 **Table 1.** Model cases description.

Name	Description
Nonvolc	No injection of volcanic H <sub>2</sub> O and SO <sub>2</sub> .
H2O_SO2	H <sub>2</sub> O and SO <sub>2</sub> injection profile follows Zhu et al. [2022].
H2O_SO2_CLO	Besides H <sub>2</sub> O and SO <sub>2</sub> , injection of 0.00013 Tg of ClO. ClO injection profile is proportional to H <sub>2</sub> O injection.



H2O_SO2_CIO_nohet	Same setting as H2O_SO2_CIO, but turn off the heterogeneous chemical reactions for HCl+HOCl, ClONO <sub>2</sub> +H <sub>2</sub> O, and ClONO <sub>2</sub> +HCl
SO2_CIO	SO <sub>2</sub> injection profile follows Zhu et al. (2022). No water injected. Injection of 0.00013 Tg of ClO using the same profile as H2O_SO2_CIO.
lowO3	Reduce the O <sub>3</sub> to 75% of its original value at 20 hPa.
H2O_SO2_lowO3	H <sub>2</sub> O and SO <sub>2</sub> injection, plus reducing O <sub>3</sub> to 75%.
H2O_SO2_CIO_lowO3	H <sub>2</sub> O, SO <sub>2</sub> and ClO injection, plus reducing O <sub>3</sub> to 75%.
H2O_SO2_NO	Injection of 0.003 Tg of NO in addition to H <sub>2</sub> O and SO <sub>2</sub> .

147

148

149

### 3. Results

150

151

152

153

154

155

156

157

158

159

160

161

162

163

164

165

166

167

168

169

170

171

172

173

174

175

176

177

178

179

180

181

*Evan et al.* [2023] show the HTHH in-plume ozone depletion at 20 hPa lasts at least ten days after the HTHH eruption, which they attribute to the heterogeneous chlorine activation on humidified volcanic aerosols. Here we analyze the contributions to this initial in-plume O<sub>3</sub> depletion considering three processes: 1) increasing H<sub>2</sub>O injection may enhance the HOx catalytic cycle and HOx/ClOx interactions; 2) increasing ClO during the injection phase may deplete ozone due to both heterogeneous reactions and gas phase reactions; 3) the rising plume from the troposphere may carry ozone-poor tropospheric air into the stratosphere.

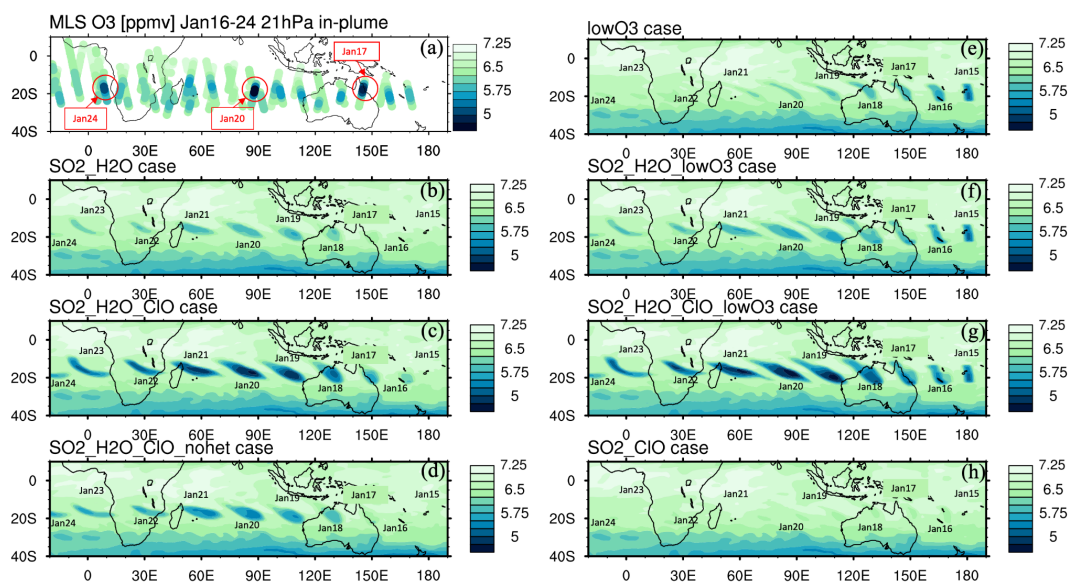
**Figure 3a** shows the MLS observed in-plume ozone depletion at 20 hPa. Because the plume is spatially small during the initial days, MLS tracks do not capture the maximum plume perturbation every day. MLS measures low ozone concentrations of 4.8 ppmv on January 17, 4.6 ppmv on January 20, and 5.1 ppmv on January 24. These are ozone anomalies of about 1.7 ppmv, 1.9 ppmv, and 1.4 ppmv, respectively. The anomalies are calculated using the background average values in this area (6.5 ppmv) subtracting the low ozone values. Note that any interpretation of these O<sub>3</sub> anomalies needs to consider the coarse MLS vertical resolution (~3 km). **Figure 3b** shows the simulated O<sub>3</sub> in the H2O\_SO2 case using one model time step each day that occurs near local noon. **Figure 3b** shows evident O<sub>3</sub> reduction, but less than observed, because of the water injection, which accelerates the HOx catalytic cycle. **Figure 3c** shows that once we inject ClO on top of the massive water injection, O<sub>3</sub> loss is significantly enhanced and is close to the observations after January 18. **Figure 3d** uses the same injection as **Figure 3c** but with heterogeneous reactions (i.e., HCl+HOCl, ClONO<sub>2</sub>+H<sub>2</sub>O, and ClONO<sub>2</sub>+HCl) turned off. The difference between **Figure 3d** and **Figure 3c** is caused by heterogeneous reactions, which usually only happen in the stratospheric polar springtime where they cause the Antarctic ozone hole and Arctic ozone depletion. Heterogeneous reactions become important, despite the high non-polar temperatures because of the massive quantity of water injected. The heterogeneous reaction rate is strongly related to the relative humidity. Usually, during the polar night, the relative humidity is higher (RH 60%-100%) than in the non-polar stratosphere because of the low temperature (<195 K). Here, the water injection increases the relative humidity (**Figure 4c**). Enhanced water causes the weight percent of H<sub>2</sub>SO<sub>4</sub> of the sulfuric acid aerosol to decrease from 70% to 35% (**Figure 4b**). The massive water injection also causes the in-plume temperature to drop about 2 to 6 K (**Figure 4f**). All these factors (temperature decrease, relative humidity increase, and particle H<sub>2</sub>SO<sub>4</sub> dilution) can increase the three heterogeneous reaction probabilities (HCl+HOCl, ClONO<sub>2</sub>+H<sub>2</sub>O, and ClONO<sub>2</sub>+HCl). As shown in **Figure 5**, when the water vapor



182 amount is near the climatological value of 6 ppmv, the heterogeneous reaction probability  
 183 reaches  $10^{-2}$  to  $10^{-1}$  when the temperature is  $\sim 190$  K. Meanwhile, the reaction probability is  
 184 similar for temperatures of 215 K when the water vapor is  $\sim 600$  ppmv in the simulations, as was  
 185 the case for the HTHH plume during the week following the eruption. COSMIC-2 radio  
 186 occultation observed even higher water vapor during the first week: the maximum values over  
 187 January 20-22 are  $\sim 1000$ - $2000$  ppmv [Randel *et al.*, 2023]. Also, because the in-plume and the  
 188 out-of-plume chemical concentrations are different, we apply both conditions (solid and dashed  
 189 lines) to show how the different HCl, HOCl, and ClONO<sub>2</sub> conditions alter the HCl+HOCl and  
 190 ClONO<sub>2</sub>+HCl reactions probabilities by one order of magnitude. Volcanic sulfur injection also  
 191 increases the sulfate surface area density (**Figure 4a**) that provides extra surfaces for  
 192 heterogeneous reactions.

193 Comparing **Figure 3b** and **3c** with MLS observations, we can see that the chemical  
 194 reactions do not explain the O<sub>3</sub> loss during the first three days of the eruption (January 15 -  
 195 January 17, low O<sub>3</sub> near 160°E in MLS observation). This discrepancy suggests that the plume  
 196 contains some ozone-poor tropospheric air after the injection into the stratosphere. We ran three  
 197 cases with initial low ozone. For the low O<sub>3</sub> case (**Figure 3e**), we inject only ozone-poor air  
 198 without volcanic H<sub>2</sub>O and SO<sub>2</sub>. It shows low O<sub>3</sub> as observed during the first couple of days, but  
 199 ozone recovers quickly because the O<sub>3</sub> chemical lifetime is short at 20 hPa inside the plume  
 200 (**Figure A4**). The H<sub>2</sub>O\_SO<sub>2</sub>\_lowO<sub>3</sub> case (**Figure 3f**) shows ozone loss similar to the  
 201 observation in the first six or seven days. By adding the ClO and initial ozone-poor air (**Figure**  
 202 **3g**), we obtain persistent low O<sub>3</sub> values that agree with the observational lowest values better  
 203 than the other cases (**Figure 6a**). Compared with **Figure 3b**, **Figure 3d** has slightly more ozone  
 204 depletion, indicating that the extra chlorine injection impacts O<sub>3</sub> even without heterogeneous  
 205 chemistry. However, without including the high amounts of injected water, the additional ClO  
 206 alone cannot deplete ozone much (**Figure 3h**).

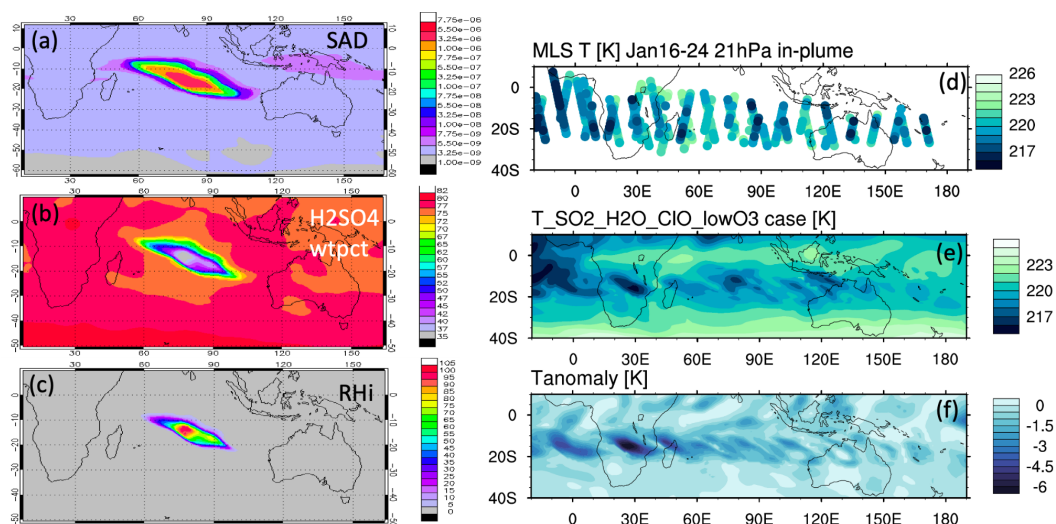
207



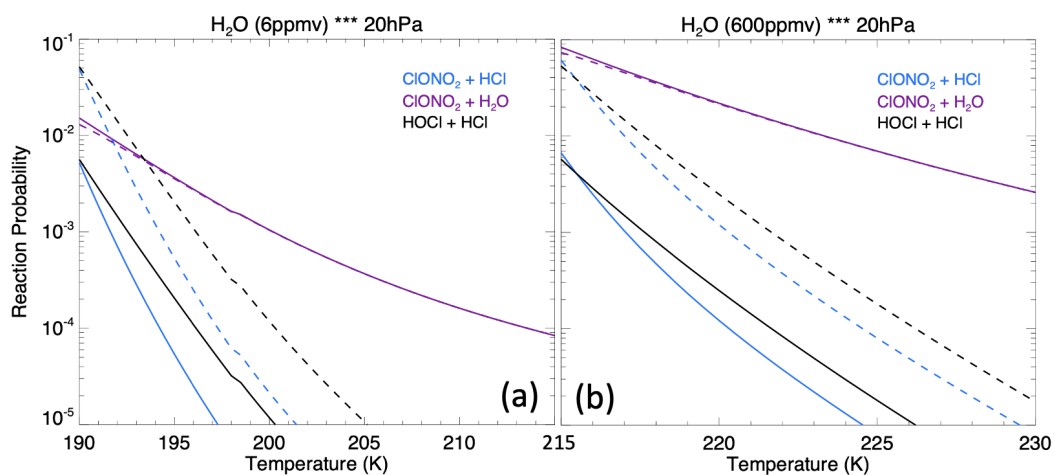
208



209 **Figure 3.** a) MLS in-plume O<sub>3</sub> observation during the first ten days. The locations and days  
 210 with low O<sub>3</sub> values used in **Figure 6** are marked with circles. b-h) Simulated 10-day evolution of  
 211 in-plume O<sub>3</sub> in seven model cases with various injections of SO<sub>2</sub>, H<sub>2</sub>O, ClO, and low initial O<sub>3</sub>.  
 212



213 **Figure 4.** a) Simulated surface area density, b) simulated H<sub>2</sub>SO<sub>4</sub>/H<sub>2</sub>O weight percent and c)  
 214 relative humidity on January 20 at 20 hPa. d) Temperature evolution during the first ten days at  
 215 20 hPa from MLS, e) simulated temperature evolution in the SO<sub>2</sub>\_H<sub>2</sub>O\_ClO\_lowO<sub>3</sub> case; f)  
 216 temperature difference between the SO<sub>2</sub>\_H<sub>2</sub>O\_ClO\_lowO<sub>3</sub> case and the Nonvolc case.  
 217  
 218



219 **Figure 5.** The heterogeneous reaction probability for three reactions on sulfate surfaces  
 220 (ClONO<sub>2</sub>+HCl, ClONO<sub>2</sub>+ H<sub>2</sub>O and HOCl+HCl) as a function of water vapor assuming 0.4 μm  
 221 particle size at 20 hPa. Panel a) assumes 6 ppmv of ambient water vapor and panel b) assumes  
 222 600 ppmv of ambient water vapor. The solid lines use the out-of-plume chemical concentration  
 223 on January 20: 1.0 ppbv of HCl, 0.03 ppbv of HOCl, and 0.5 ppbv of ClONO<sub>2</sub>; the dashed lines  
 224



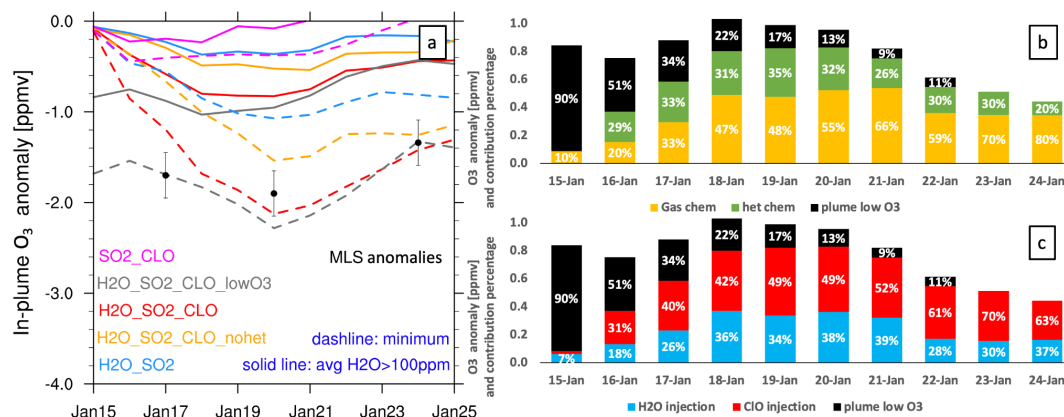
225 use the in-plume chemical concentration: 0.1 ppbv of HCl, 1.0 ppbv of HOCl, and 0.05 ppbv of  
 226 ClONO<sub>2</sub>. These values are based on the simulation output.

227  
 228 **Figure 6** shows the O<sub>3</sub> anomaly evolution from several model cases (**a**) and percentage  
 229 contributions to the total ozone loss (**b, c**). The model case with all injections (initial low O<sub>3</sub>,  
 230 high H<sub>2</sub>O, and high ClO) agrees well with MLS observations on the three days with the lowest  
 231 O<sub>3</sub> values (**Figure 6a**). In **Figure 6b** and **6c**, the black bars represent the contribution from the  
 232 low O<sub>3</sub> injection, which is significant during the first couple of days but diminishes quickly.  
 233 From these percentage values, we conclude that the low O<sub>3</sub> carried in the plume lofting cannot be  
 234 the reason for the low O<sub>3</sub> values after 3 days. Chemistry is the main reason that this O<sub>3</sub> depletion  
 235 lasts so long.

236 There are two ways to look at the chemical contributors to ozone loss based on our model  
 237 runs. The first is to separate the contributors due to various injections (**Figure 6c**): H<sub>2</sub>O injection  
 238 accounts for about 30-40% of the ozone loss most of the time (blue) and ClO injection accounts  
 239 for 50% of the ozone loss most of the time (red). However, we cannot simply attribute the largest  
 240 contribution to the ClO injection, because if we only inject ClO, it does not produce much ozone  
 241 depletion (**Figure 6a**, magenta). It is the ClO<sub>x</sub>/HO<sub>x</sub> interactions that accelerate O<sub>3</sub> depletion.

242 A second way to look at the causes for ozone loss is to separate the contributions from  
 243 the gas-phase chemistry and the heterogeneous chemistry (**Figure 6b**). The model run with the  
 244 H<sub>2</sub>O and ClO injections, but without the heterogeneous chemistry shows that the gas-phase  
 245 chemistry (yellow bars) account for more than 47% of the ozone loss from January 18 - 24.  
 246 Heterogeneous chemistry (green bars) destroys about 30% of the ozone. Hence, both  
 247 heterogeneous chemistry and gas-phase chemistry are important for O<sub>3</sub> depletion. Once we turn  
 248 off the heterogeneous chemistry, the partitioning between active chlorine and chlorine in the  
 249 reservoirs is changed. The order in which the processes are accounted for can affect the resulting  
 250 breakdown. Thus, we cannot simply say that gas phase chemistry contributions are larger than  
 251 heterogeneous chemistry. Both are clearly significant.

252



253 **Figure 6. a)** O<sub>3</sub> anomaly in different model cases. The solid lines are the average O<sub>3</sub> anomaly at  
 254 20 hPa on each day near local noon where water vapor is larger than 100 ppmv. 100 ppmv here  
 255 is suggested by *Evan et al.* [2023], who found that O<sub>3</sub> anomalies are not significant for a 10  
 256 ppmv but significant for a 100 ppmv threshold. The dashed lines are the simulated maximum O<sub>3</sub>  
 257 anomaly on each day at 20 hPa. The black dots show the three days during which MLS measures  
 258





259 the lowest O<sub>3</sub> values (explained in **Figure 3a**). **b**) The percentage contributions to ozone loss  
260 from gas phase chemistry (orange) (H<sub>2</sub>O\_SO<sub>2</sub>\_CLO\_nohet), heterogeneous chemistry (green,  
261 H<sub>2</sub>O\_SO<sub>2</sub>\_CLO minus H<sub>2</sub>O\_SO<sub>2</sub>\_CLO\_nohet), and low O<sub>3</sub> air carried into the stratosphere  
262 (black, H<sub>2</sub>O\_SO<sub>2</sub>\_CLO\_lowO<sub>3</sub> minus H<sub>2</sub>O\_SO<sub>2</sub>\_CLO). **c**) The percentage contributions to  
263 ozone loss from H<sub>2</sub>O injection (blue, H<sub>2</sub>O\_SO<sub>2</sub> minus Nonvolc), ClO injection (red,  
264 H<sub>2</sub>O\_SO<sub>2</sub>\_CLO minus H<sub>2</sub>O\_SO<sub>2</sub>), and low O<sub>3</sub> air carried into the stratosphere (black,  
265 H<sub>2</sub>O\_SO<sub>2</sub>\_CLO\_lowO<sub>3</sub> minus H<sub>2</sub>O\_SO<sub>2</sub>\_CLO).  
266

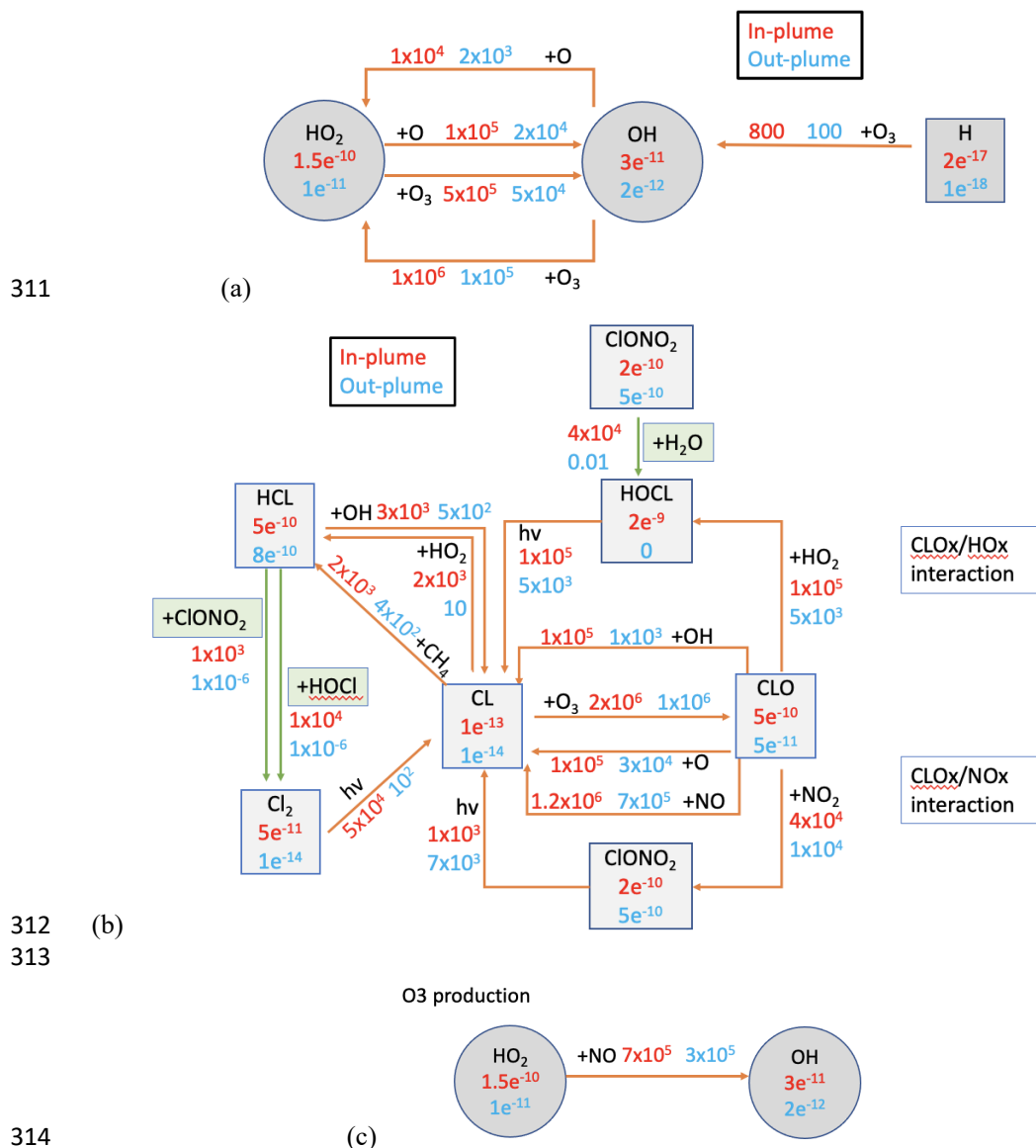
267 To better understand which reactions are critical in the HTHH plume, we investigate the  
268 simulated reaction rates related to HO<sub>x</sub> and chlorine compounds (**Figure 7**). These reactions  
269 reflect how the water and ClO injections strengthen the in-plume HO<sub>x</sub>/ClO<sub>x</sub> interactions,  
270 chlorine activation, and the relative importance of each heterogeneous reaction rate. The  
271 WACCM model uses the methods developed by *Shi et al.* [2001] for heterogeneous reaction rate  
272 calculations. **Figure 7a** shows the HO<sub>x</sub> cycle inside and outside the water plume on January 20,  
273 daytime, at 20 hPa. The HO<sub>2</sub>+O<sub>3</sub> reaction rate increases from 5x10<sup>4</sup> to 5x10<sup>5</sup> cm<sup>-3</sup>sec<sup>-1</sup>; OH+O  
274 increases from 2x10<sup>4</sup> to 10<sup>5</sup> cm<sup>-3</sup>sec<sup>-1</sup>; HO<sub>2</sub>+O increases from 2x10<sup>3</sup> to 10<sup>4</sup> cm<sup>-3</sup>sec<sup>-1</sup>. In addition,  
275 the extra HO<sub>x</sub> plays a large role in chlorine activation. **Figure 7b** shows the chlorine compound  
276 reactions inside the HTHH initial plume. The HOCl photolysis rate increases from 5x10<sup>3</sup>  
277 cm<sup>-3</sup>sec<sup>-1</sup> outside the plume to 10<sup>5</sup> cm<sup>-3</sup>sec<sup>-1</sup> inside the plume, which is the dominant process  
278 causing the increase in chlorine activation to Cl. The HOCl concentration remains high due to  
279 the enhanced ClO<sub>x</sub>/HO<sub>x</sub> interaction (i.e., ClO+HO<sub>2</sub>→HOCl+O<sub>2</sub> reaction), as well as the increase  
280 of the heterogeneous reaction rate of ClONO<sub>2</sub>+H<sub>2</sub>O from 10<sup>-2</sup> to 4x10<sup>4</sup> cm<sup>-3</sup>sec<sup>-1</sup>. The large  
281 amounts of HOCl also make the heterogeneous reaction of HOCl+HCl faster than the  
282 ClONO<sub>2</sub>+HCl reaction, while the latter reaction is known as the major reaction contributing to  
283 the chlorine activation that contributes to the polar ozone depletion. **Figure A5** shows the uptake  
284 coefficient for the three heterogeneous reactions HCl+HOCl, ClONO<sub>2</sub>+H<sub>2</sub>O, and ClONO<sub>2</sub>+HCl  
285 on January 20. The reaction rate of ClONO<sub>2</sub>+HCl is increased to 10<sup>-2</sup> cm<sup>-3</sup>sec<sup>-1</sup> compared with  
286 the background value of 10<sup>-10</sup> cm<sup>-3</sup>sec<sup>-1</sup>. This value is even higher than *Evan et al.* [2023]  
287 suggested, who estimate that enhanced water increases the uptake coefficient of ClONO<sub>2</sub>+HCl to  
288 10<sup>-4</sup> cm<sup>-3</sup>sec<sup>-1</sup>. The reaction probability of HCl+HOCl and ClONO<sub>2</sub>+H<sub>2</sub>O increases to 10<sup>-2</sup> cm<sup>-3</sup>  
289 sec<sup>-1</sup>. Furthermore, inside the plume, the reactions that convert Cl back to HCl are slower than  
290 their activation rate.

291 **Figure 7c** shows another process significantly altered by the water plume. HO<sub>2</sub>+NO is  
292 usually not an important process for O<sub>3</sub> production in the stratosphere (more important in the  
293 troposphere). The reaction rate increases from 3x10<sup>5</sup> cm<sup>-3</sup>sec<sup>-1</sup> outside the plume to 7x10<sup>5</sup> cm<sup>-3</sup>  
294 sec<sup>-1</sup> inside the plume.

295 **Figure 8** shows the contributions to Cly  
296 (Cl+ClO+2Cl<sub>2</sub>+2Cl<sub>2</sub>O<sub>2</sub>+OCIO+HOCl+ClONO<sub>2</sub>+HCl+BrCl) and the percentage of each  
297 compound inside and outside the plume. Outside the plume, HCl and ClONO<sub>2</sub> are dominant,  
298 indicating that most of the Cl is in reservoirs. While inside the water plume, both the H<sub>2</sub>O\_SO<sub>2</sub>  
299 and H<sub>2</sub>O\_SO<sub>2</sub>\_CLO cases show strong depletion of the reservoirs HCl and ClONO<sub>2</sub>, and most of  
300 the Cly is either in the form of HOCl (a short-lived reservoir) or is activated in the form of ClO.  
301 Unlike the chlorine activation process in the polar winter, HOCl is the highest in the HTHH  
302 plume because heterogeneous chemistry is not fast enough to destroy HOCl to produce ClO. In  
303 the case without heterogeneous chemistry, HCl and ClONO<sub>2</sub> are dominant in the plume,  
304 indicating that heterogeneous chemistry is the main process of converting HCl to active chlorine.



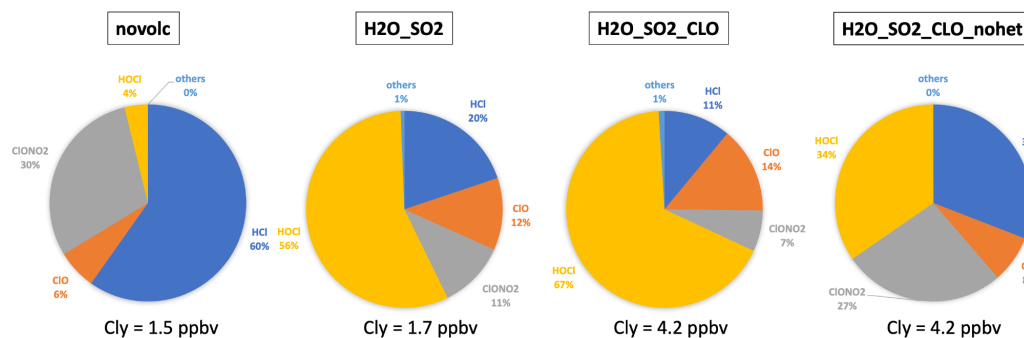
305 Comparing total Cly and ClO in all panels, ClO does not exceed a quarter of the Cly, indicating  
 306 adding 0.00013Tg of ClO through injection is one way to produce the observed ClO. There is a  
 307 possibility that ClO is converted from other Cly species through chemical reactions we are not  
 308 aware of because this was a very unusual eruption.  
 309  
 310



315 **Figure 7.** Reactions inside and outside the plume in  $\text{cm}^{-3}\text{sec}^{-1}$  and compound concentrations in  
 316 mol/mol. Red numbers represent values inside the plume, blue numbers outside the plume. **a)**  
 317 HOx balance and its interaction with Ox during daytime at 20 hPa on January 20, 2022. **b)**



318 Chlorine compound reactions in the H<sub>2</sub>O\_SO<sub>2</sub>\_ClO case. **c)** HO<sub>x</sub> cycle impact on O<sub>3</sub>  
 319 production. Green arrows represent the heterogeneous reactions for chlorine activation. H<sub>2</sub>O is ~  
 320 600 ppm inside the plume and ~5.5 ppm outside the plume. Cly is ~ 4.2 ppbv inside the plume  
 321 and 1.5 ppbv outside the plume.  
 322



323  
 324 **Figure 8.** The percentage of each inorganic chlorine compound  
 325 (Cly=Cl+ClO+2Cl<sub>2</sub>+2Cl<sub>2</sub>O<sub>2</sub>+OCIO+HOCl+ClONO<sub>2</sub>+HCl+BrCl) inside and outside the plume.  
 326 The slight difference between novolc Cly and H<sub>2</sub>O\_SO<sub>2</sub> Cly is because H<sub>2</sub>O injection changes  
 327 the plume dynamics in the free-running simulations.  
 328

#### 329 4. Discussion

330 The ozone loss inside the HTHH plume during the first ten days provides a unique  
 331 opportunity to study stratospheric chemistry and to understand the performance of the WACCM  
 332 state-of-the-art climate model, because the HTHH injected ClO and H<sub>2</sub>O exceed the normal  
 333 range of the stratospheric variability. These volcanic injections strongly altered the ClO<sub>x</sub>/HO<sub>x</sub>  
 334 interactions and heterogeneous reaction rates, producing different chemical pathways for  
 335 chlorine activation and ozone depletion from what occurs in the Antarctic ozone hole or Arctic  
 336 ozone depletion in the polar stratospheric winter and spring. HOCl is identified as playing a large  
 337 role in the in-plume chlorine balance and heterogeneous processes. The high HOCl  
 338 concentrations are a result of the very high in-plume water vapor content, which makes this event  
 339 different from chemistry in the Antarctic ozone hole, where ClONO<sub>2</sub> is more important.

340 This study also raises an interesting question of where the Cl comes from in the volcanic  
 341 injection. Seawater contains 3.5% sea salt, which implies that about 5 Tg of NaCl could have  
 342 been injected assuming that the injected 150 Tg of H<sub>2</sub>O came from sea water. However, we only  
 343 need to inject 0.00013 Tg of ClO to match the MLS ClO observations during the first few days  
 344 after the eruption. We also conducted a test injecting an equivalent amount of HCl (0.0009 Tg),  
 345 which resulted in a similar HOCl, ClO, and O<sub>3</sub> pattern (**Figure A2 and A3**). If we inject more  
 346 HCl or ClO, ClO would exceed the observed concentration, causing depletion of OH, and  
 347 slowing down the SO<sub>2</sub> oxidation. Evidently, if the water came from seawater, most NaCl was not  
 348 converted to HCl but stayed in the stratosphere as particles. Vernier *et al.* [2023] sampled NaCl  
 349 particles eight months after the eruption near Brazil. Based on their sampled NaCl concentration,  
 350 we estimate 0.5 to 1 Tg of NaCl may have been injected and stayed in the atmosphere. There are  
 351 several possibilities why this event did not inject 5 Tg of NaCl in the stratosphere: Remote  
 352 sensing particle size estimations [Khaykin *et al.*, 2022] and in-situ measurements [Asher *et al.*,  
 353 2023] indicates that the particles were submicron sized. However, sea salt particles injected into



354 the lower troposphere by wind are mainly particles larger than 10  $\mu\text{m}$ . Hence, if the volcanic  
 355 injection had similar sized NaCl particles, most of them may have quickly fallen out of the  
 356 stratosphere. In addition, the majority of NaCl might have been washed out during the first  
 357 couple of hours of plume injection by acting as nuclei for ice particles. It is also possible that the  
 358 reactions that might release Cl from NaCl may not efficiently lead to reactive Cl. For example,  
 359  $\text{HNO}_3$  can react on sea salt heterogeneously very quickly in the troposphere to release HCl (De  
 360 Haan and Finlayson-Pitts, 1997; Guimbaud et al., 2002; Murphy et al., 2019). This reaction may  
 361 be accelerated by HTHH high humidity even if the temperature is low in the stratosphere. HCl  
 362 could be removed by condensing in supercooled water, which would reduce HCl vapor  
 363 concentrations by up to four orders of magnitude, preventing substantial stratospheric chlorine  
 364 injection [Tabazadeh and Turco, 1993]. Finally, it may be that the water injected came from  
 365 magmatic water, or seawater that percolated into the volcano and was released as steam. Such  
 366 water would not be rich in NaCl. In that case Cl observed by Vernier et al. [2023] may have been  
 367 bound up in minerals of the volcanic ash. Other halogen species such as bromine and iodine are  
 368 often observed after volcanic eruptions (large amounts of BrO were observed after HTHH in the  
 369 troposphere [Li et al., 2023]). However, they can lead to much stronger ozone depletion if they  
 370 persist in the stratosphere. Since the elevated Cl in the model can well explain the  $\text{O}_3$  depletion,  
 371 the impact of bromine and iodine on stratospheric  $\text{O}_3$  is minimal for this eruption.

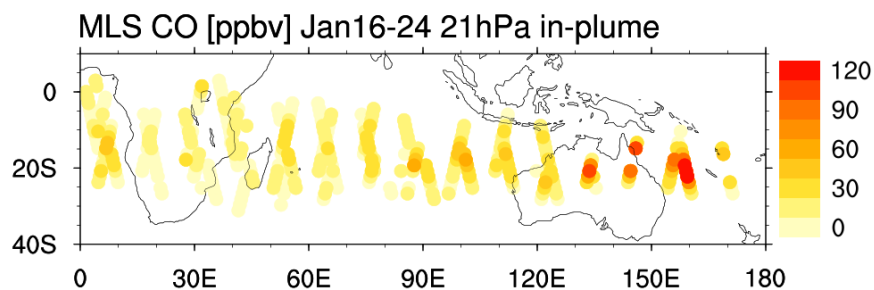
372 In addition,  $\text{NO}_x$  can be produced by lightning inside or around the volcanic plume.  
 373 Observations show there was a record number of lightning events in this volcanic plume. Almost  
 374 400,000 flashes were observed by the GLD360 network over the 6 hours of the most active  
 375 eruption period (and ~590,000 total flashes) [Global Volcanism Program, 2022]. Considering  
 376 that tropospheric global models use a lightning source of 5 Tg(N)/yr and an average flash the  
 377 OTD/LIS satellite sensors produced an average global flash rate of  $44 \pm 5$  flashes per second, an  
 378 injection of N of ~0.001- 0.003 Tg (0.002 - 0.006 Tg of NO) would be expected for the HTHH  
 379 eruption. We conducted a model run with  $\text{H}_2\text{O}$ ,  $\text{SO}_2$ , and an injection of 0.003 Tg of NO,  
 380 showing that this additional NO has little impact on the  $\text{O}_3$  loss and ClO levels during the first  
 381 ten days (**Figure A6**). Therefore, lightning  $\text{NO}_x$  probably does not contribute to the HTHH initial  
 382 in-plume  $\text{O}_3$  loss. Because of the high water, NO would convert to  $\text{HNO}_3$  in the first couple of  
 383 days. Unfortunately, we lack observations of  $\text{HNO}_3$ , NO, or  $\text{NO}_2$  right after the eruption. MLS  
 384 observations in February (**Figure A7**) and the model simulations with  $\text{H}_2\text{O}$  injection or  $\text{H}_2\text{O}+\text{NO}$   
 385 injections show elevated  $\text{HNO}_3$  compared with the background.

386

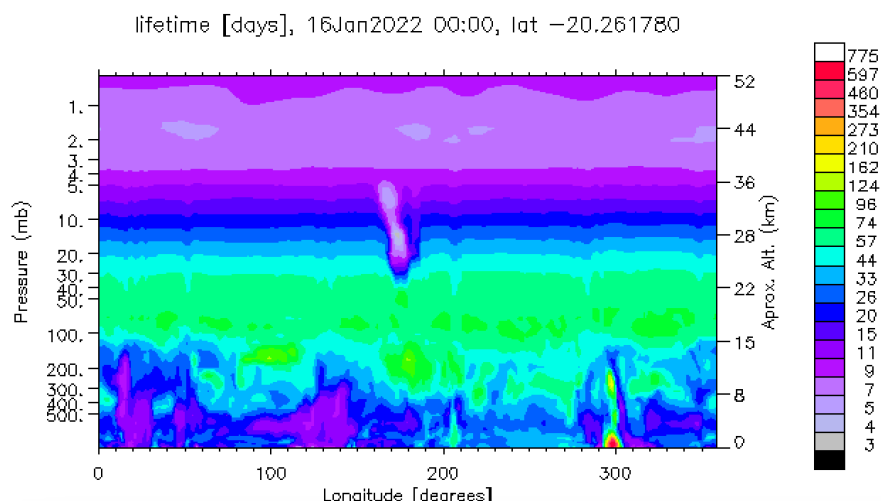
387

388 **Appendix A**

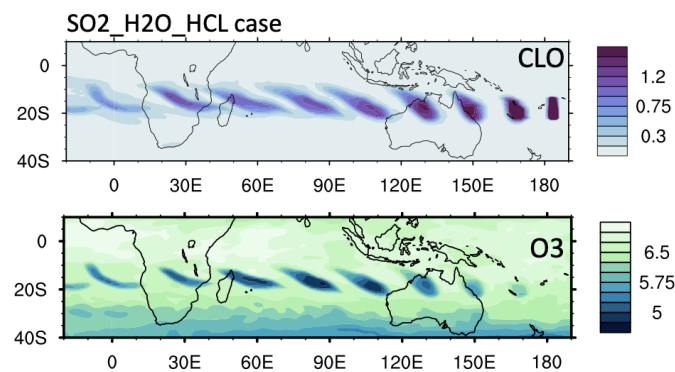
389



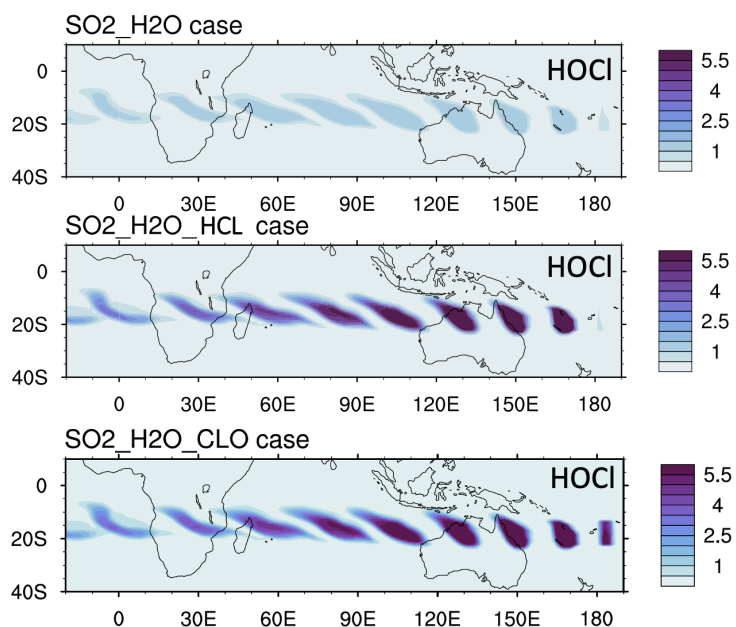
390



391  
 392 **Figure A1.** Top panel shows the MLS in-plume CO observation during the first 10 days after the  
 393 eruption. The bottom panel shows the CO lifetime on Jan 16 at 20°S is shortened from a month  
 394 to a few days because of the volcanic water plume. The observed CO mixing ratios of around  
 395 120 ppmv seem incompatible with typical CO levels over oceanic regions, indicating the  
 396 production of CO within the magma chamber or in the hot plume itself.  
 397



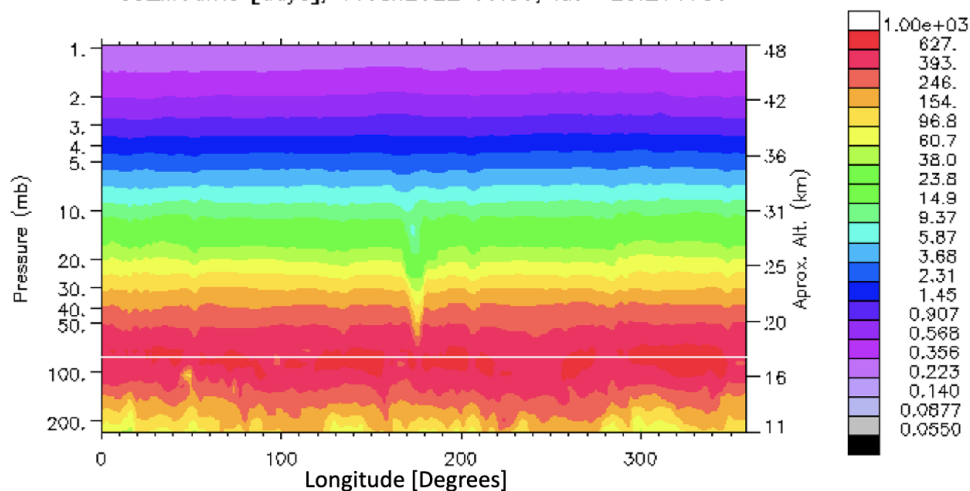
398  
 399 **Figure A2.** The O<sub>3</sub> and CIO evolution from the model case with an HCl injection of 0.000092  
 400 Tg (equivalent to 0.00013 Tg of CIO injection).  
 401



402  
403

**Figure A3.** The HOCl evolution from the three model cases.

O3\_lifetime [days], 16Jan2022 00:00, lat -20.261780



404  
405  
406  
407

**Figure A4.** O<sub>3</sub> chemical lifetime is about 1 to 2 months at 20 hPa and is reduced to 10 days at the HTHH location.



408  
409  
410  
411

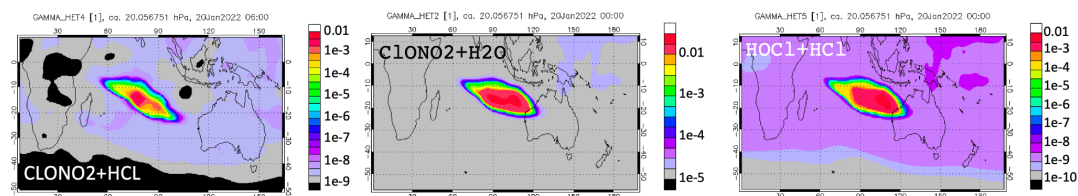


**Figure A5.** Heterogeneous reaction probabilities for the three heterogeneous reactions on January 20 at 20 hPa.

412  
413  
414  
415

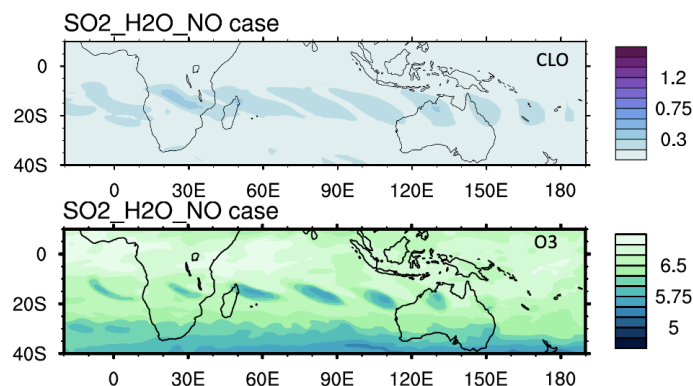
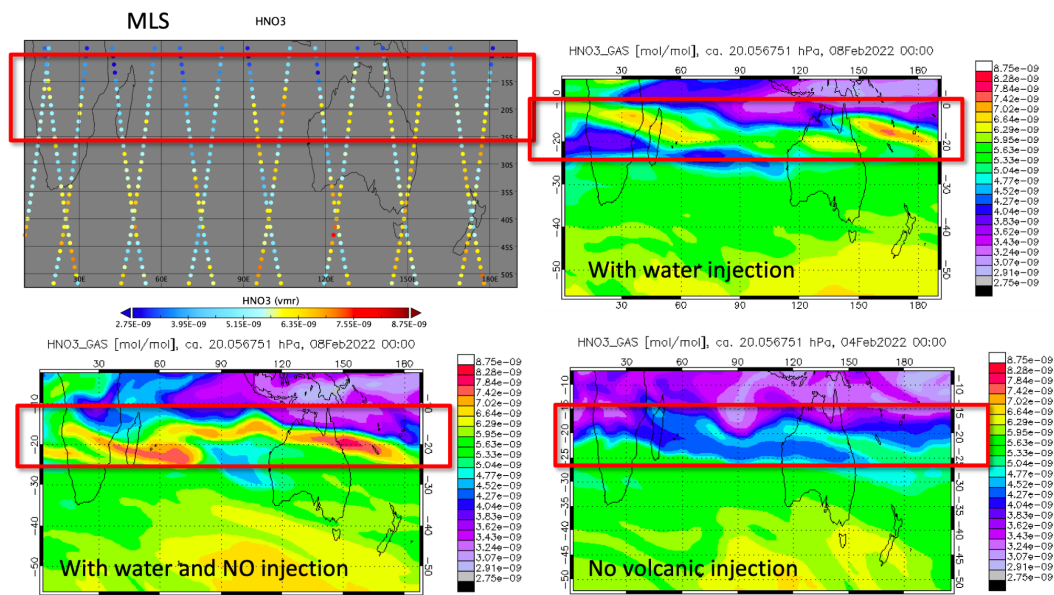


**Figure A6.** O<sub>3</sub> and ClO evolution from the model case with NO injection of 0.003 Tg, which is identical to the SO<sub>2</sub>\_H<sub>2</sub>O case. The ClO and O<sub>3</sub> enhancement are due to the H<sub>2</sub>O injection.

416





417 **Figure A7.** HNO<sub>3</sub> observed by MLS on February 8, 2022 compared to the model simulation  
418 with water and NO injection, as well as the no volcanic injection case. MLS shows similar  
419 elevated HNO<sub>3</sub> as the simulation case with H<sub>2</sub>O injection or with H<sub>2</sub>O/NO injection.

420

421

422

423 **Code availability:** The CESM2 model is available on the CESM trunk to any registered user at  
424 [www.cesm.ucar.edu](http://www.cesm.ucar.edu).

425 **Data availability:** The main simulation data generated during this study are available at  
426 (<https://osf.io/f69ns/>) with a permanent DOI 10.17605/OSF.IO/F69NS. Aura MLS v4 data is  
427 available at <https://disc.gsfc.nasa.gov/datasets?page=1&keywords=AURA%20MLS>. Water  
428 vapor radiosonde data is available at <https://doi.org/10.5065/p328-z959> (26).

429 **Author contribution:** YZ, RWP, DK, and KHR designed the experiments and YZ performed  
430 the simulations. YZ prepared the manuscript with contributions from all co-authors. DK  
431 examined the sensitivity of the stratospheric H<sub>2</sub>O abundance on the reaction probability (Figure  
432 5). LM, HV and SE provided observational data and analysis. RWP, DK, OBT, JZ, ST, CGB,  
433 XW, WJR and KHR participated in the modeling data analysis.

434 **Competing interests:** At least one of the (co-)authors is a member of the editorial board  
435 of Atmospheric Chemistry and Physics.

436

#### 437 **Acknowledgement**

438 This project received funding from NOAA's Earth Radiation Budget (ERB) Initiative  
439 (CPO #03-01-07-001). This research was supported in part by NOAA cooperative agreements  
440 NA17OAR4320101 and NA22OAR4320151. We thank Hazel Vernier, Dr. Kimberlee Dube, Dr.  
441 Pengfei Yu, Fracis Vitt, Dr. Ru-shan Gao, Dr. Margaret Tolbert, Dr. Micheal Mills, Dr. Daniel  
442 Murphy, and Dr. Brian Ridley for their valuable input. NCAR's Community Earth System  
443 Model project is supported primarily by the National Science Foundation. This material is based  
444 upon work supported by the National Center for Atmospheric Research, which is a major facility  
445 sponsored by the NSF under Cooperative Agreement No. 1852977. Computing and data storage  
446 resources, including the Cheyenne supercomputer (doi:10.5065/D6RX99HX), were provided by  
447 the Computational and Information Systems Laboratory (CISL) at NCAR. Work at the Jet  
448 Propulsion Laboratory, California Institute of Technology, was carried out under a contract with  
449 the National Aeronautics and Space Administration (80NM0018D0004).

450

451

452 **Reference:**

453





- 454 Anderson, J. G., D. M. Wilmouth, J. B. Smith, and D. S. Sayres (2012), UV Dosage Levels in  
455 Summer: Increased Risk of Ozone Loss from Convectively Injected Water Vapor, *Science*,  
456 337(6096), 835-839, doi: <https://doi.org/10.1126/science.1222978>.
- 457 Asher, E., Todt, M., Rosenlof, K.H., Thornberry, T.D., Gao, R.S., Taha, G., Walter, P.J.,  
458 Alvarez, S.L., Flynn, J., Davis, S.M. and Evan, S., (2022). The unprecedented rapid aerosol  
459 formation from the Hunga Tonga-Hunga Ha'apai eruption. AGU Fall Meeting Abstracts  
460 (Vol. 2022, pp. A42I-01).
- 461 De Haan, D. O.; Finlayson-Pitts, B. J. Knudsen cell studies of the reaction of gaseous nitric acid  
462 with synthetic sea salt at 298 K. *J. Phys. Chem. A* 1997, 101, 9993-9999,  
463 doi:10.1021/jp972450s.
- 464 Evan et al., (2023), Rapid ozone loss following humidification of the stratosphere by the Hunga  
465 Tonga Eruption, submitted to *Science*. Cited with authors' permission.
- 466 Global Volcanism Program, 2022. Report on Hunga Tonga-Hunga Ha'apai (Tonga). In: Sennert,  
467 S K (ed.), *Weekly Volcanic Activity Report*, 12 January-18 January 2022. Smithsonian  
468 Institution and US Geological Survey.
- 469 Guimbaud, C.; Arens, F.; Gutzwiller, L.; Gäggeler, H. W.; Ammann, M. Uptake of HNO<sub>3</sub> to  
470 deliquescent sea-salt particles: a study using short-lived radioactive isotope tracer <sup>13</sup>N.  
471 *Atmos. Chem. Phys.* 2002, 2, 249-257, doi:10.5194/acp-2-249-2002.
- 472 Hofmann, D. J., and S. J. Oltmans (1993), Anomalous Antarctic ozone during 1992: Evidence  
473 for Pinatubo volcanic aerosol effects, *Journal of Geophysical Research: Atmospheres*,  
474 98(D10), 18555-18561, doi:<https://doi.org/10.1029/93JD02092>.
- 475 Khaykin, S., et al. (2022), Global perturbation of stratospheric water and aerosol burden by  
476 Hunga eruption, *Communications Earth & Environment*, 3(1), 316, doi:10.1038/s43247-022-  
477 00652-x.
- 478 Kinnison, D. E., K. E. Grant, P. S. Connell, D. A. Rotman, and D. J. Wuebbles (1994), The  
479 chemical and radiative effects of the Mount Pinatubo eruption, *Journal of Geophysical  
480 Research: Atmospheres*, 99(D12), 25705-25731, doi: <https://doi.org/10.1029/94JD02318>.
- 481 Li, Q., Qian, Y., Luo, Y., Cao, L., Zhou, H., Yang, T., ... & Liu, W. (2023). Diffusion Height and  
482 Order of Sulfur Dioxide and Bromine Monoxide Plumes from the Hunga Tonga–Hunga  
483 Ha'apai Volcanic Eruption. *Remote Sensing*, 15(6), 1534.
- 484 Livesey, N., J., Read, W. G., Wagner, P. A., Froidevaux, L., Santee, M. L., Schwartz, M. J., et  
485 al. (2022), Version 5.0x Level 2 and 3 data quality and description document (Tech. Rep.  
486 No.JPL D-105336 Rev. B). Jet Propulsion Laboratory, Retrieved from  
487 [https://mls.jpl.nasa.gov/data/v5-0\\_data\\_quality\\_document.pdf](https://mls.jpl.nasa.gov/data/v5-0_data_quality_document.pdf)
- 488 Millán, L., et al. (2022), The Hunga Tonga-Hunga Ha'apai Hydration of the Stratosphere,  
489 *Geophysical Research Letters*, 49(13), e2022GL099381,  
490 doi:<https://doi.org/10.1029/2022GL099381>.
- 491 Murphy, D. M., Froyd, K. D., Bian, H., Brock, C. A., Dibb, J. E., DiGangi, J. P., ... & Yu, P.  
492 (2019). The distribution of sea-salt aerosol in the global troposphere. *Atmospheric Chemistry  
493 and Physics*, 19(6), 4093-4104.
- 494 Portmann, R. W., S. Solomon, R. R. Garcia, L. W. Thomason, L. R. Poole, and M. P.  
495 McCormick (1996), Role of aerosol variations in anthropogenic ozone depletion in the polar  
496 regions, *Journal of Geophysical Research: Atmospheres*, 101(D17), 22991-23006,  
497 doi:<https://doi.org/10.1029/96JD02608>.



- 498 Randel, W. J., Johnston, B. R., Braun, J. J., Sokolovskiy, S., Vömel, H., Podglajen, A., & Legras,  
499 B. (2023). Stratospheric Water Vapor from the Hunga Tonga–Hunga Ha’apai Volcanic  
500 Eruption Deduced from COSMIC-2 Radio Occultation. *Remote Sensing*, 15(8), 2167.  
501 Rienecker, M. M. et al. The GEOS-5 Data Assimilation System: Documentation of Versions 5.0.  
502 1, 5.1. 0, and 5.2. 0 (2008).  
503 Shi, Q., J. T. Jayne, C. E. Kolb, D. R. Worsnop, and P. Davidovits (2001), Kinetic model for  
504 reaction of ClONO<sub>2</sub> with H<sub>2</sub>O and HCl and HOCl with HCl in sulfuric acid solutions,  
505 *Journal of Geophysical Research: Atmospheres*, 106(D20), 24259-24274,  
506 doi:<https://doi.org/10.1029/2000JD000181>.  
507 Solomon, S., S. Borrmann, R. R. Garcia, R. Portmann, L. Thomason, L. R. Poole, D. Winker,  
508 and M. P. McCormick (1997), Heterogeneous chlorine chemistry in the tropopause region,  
509 *Journal of Geophysical Research: Atmospheres*, 102(D17), 21411-21429,  
510 doi:<https://doi.org/10.1029/97JD01525>.  
511 Solomon, S., D. J. Ivy, D. Kinnison, M. J. Mills, R. R. Neely, and A. Schmidt (2016),  
512 Emergence of healing in the Antarctic ozone layer, *Science*, 353(6296), 269-274,  
513 doi:<https://doi.org/10.1126/science.aae0061>.  
514 Tabazadeh, A., and R. P. Turco (1993), Stratospheric Chlorine Injection by Volcanic Eruptions:  
515 HCl Scavenging and Implications for Ozone, *Science*, 260(5111), 1082-1086, doi:  
516 <https://doi.org/10.1126/science.260.5111.1082>.  
517 Tie, X., and G. Brasseur (1995), The response of stratospheric ozone to volcanic eruptions:  
518 Sensitivity to atmospheric chlorine loading, *Geophysical Research Letters*, 22(22), 3035-  
519 3038, doi:<https://doi.org/10.1029/95GL03057>.  
520 Vernier, H., Quintão, D., Biazon, B., Landulfo, E., Souza, G., J. S. Lopes, F., Rastogi, N.,  
521 Meena, R., Liu, H., Fadnavis, S., Mau, J., K. Pandit, A., Berthet, G., and Vernier, J.-P.:  
522 Understanding the impact of Hunga-Tonga undersea eruption on the stratospheric aerosol  
523 population using Balloon measurements, Satellite data, and model simulations, EGU General  
524 Assembly 2023, Vienna, Austria, 24–28 Apr 2023, EGU23-6882,  
525 <https://doi.org/10.5194/egusphere-egu23-6882>, 2023.  
526 Vömel, H., S. Evan, and M. Tully (2022), Water vapor injection into the stratosphere by Hunga  
527 Tonga-Hunga Ha’apai, *Science*, 377(6613), 1444-1447, doi:  
528 <https://doi.org/10.1126/science.abq2299>.  
529 Wang, X., W. Randel, Y. Zhu, S. Tilmes, J. Starr, W. Yu, R. Garcia, B. Toon, M. Park, and D.  
530 Kinnison (2022), Stratospheric climate anomalies and ozone loss caused by the Hunga Tonga  
531 volcanic eruption, *Authorea Preprints*.  
532 Yu, P., et al. (2019), Black carbon lofts wildfire smoke high into the stratosphere to form a  
533 persistent plume, *Science*, 365(6453), 587-590, doi:<https://doi.org/10.1126/science.aax1748>.  
534 Zhu, Y., et al. (2022), Perturbations in stratospheric aerosol evolution due to the water-rich  
535 plume of the 2022 Hunga-Tonga eruption, *Communications Earth & Environment*, 3(1), 248,  
536 doi:10.1038/s43247-022-00580-w.  
537